Electronic Supplementary Information on

$[SMe_3]_2[Bi_2Ag_2I_{10}]$, a Silver Iodido Bismuthate with an Unusually Small Band Gap

Jakob Möbs[1], Sudip Pan[2], Ralf Tonner-Zech[2] and Johanna Heine[1,*]

[1] Department of Chemistry and Material Sciences Center, Philipps-Universität Marburg, Hans-Meerwein-Straße. 35043 Marburg, Germany; johanna.heine@chemie.uni-marburg.de

[2] Wilhelm-Ostwald-Institut für Physikalische und Theoretische Chemie, Fakultät für Chemie und Mineralogie, Universität Leipzig, Linnéstraße 2, 04103 Leipzig, Germany

Table of contents

Additional crystallographic details

Single crystal X-ray determination was performed on a STOE STADIVARI diffractometer with microfocus CuK_α radiation and a Pilatus 300K (Dectris) detector or a STOE IPDS2 diffractometer equipped with an imaging plate detector system using parallel beam MoK_α radiation with graphite monochromatization.

Table S1: Crystallographic data for **1**, measured on a STOE STADIVARI at 100 K, CCDC 2182488.

	1
Empirical formula	$C_3H_9AgBiI_5S$
Formula weight	1028.51
Temperature/K	100
Crystal system	monoclinic
Space group	$P2_1/n$
a/Å	8.4976(15)
b/Å	17.660(3)
c/Å	10.9308(19)
α/°	90
β/°	92.046(14)
γ/°	90
Volume/Å^3	1639.3(5)
Z	4
ρcalcg/cm^3	4.167
μ/mm^{-1}	105.225
Absorption correction (T_{min}/T_{max})	multi-scan (0.126/0.524)
F(000)	1752.0
Crystal size/mm^3	0.03362 × 0.01281 × 0.00706
Radiation	CuK_α (λ = 1.54186)
2Θ range for data collection/°	9.52 to 151.024
Index ranges	-10 ≤ h ≤ 10, -22 ≤ k ≤ 22, -6 ≤ l ≤ 13
Reflections collected	16999
Independent reflections	3345 [R_{int} = 0.0522, R_{sigma} = 0.0410]
Data/restraints/parameters	3345/3/113
Goodness-of-fit on F^2	1.032
Final R indexes [I>=2σ (I)]	R_1 = 0.0425, wR_2 = 0.0982
Final R indexes [all data]	R_1 = 0.0633, wR_2 = 0.1084
Largest diff. peak/hole / e Å^{-3}	2.64/-1.65

Details of crystal structure measurement and refinement: The $[SMe_3]^+$-cation shows a disorder at the sulfur atom over two positions. These were modeled as two parts and refined to occupancies of 27.5(12) % and 72.5(12) %. SADI restraints were used on the carbon-sulfur distances to ensure a stable

refinement. All non-hydrogen atoms were refined anisotropically. Hydrogen atoms were assigned to idealized geometric positions and included in structure factors calculations. After the final refinement a relatively large residue electron density of 2.64 e $Å^{-3}$ close to the silver position is observed. However this can be explained as an artifact of the very high x-ray absorption of the compound of 105.2 mm^{-1}.

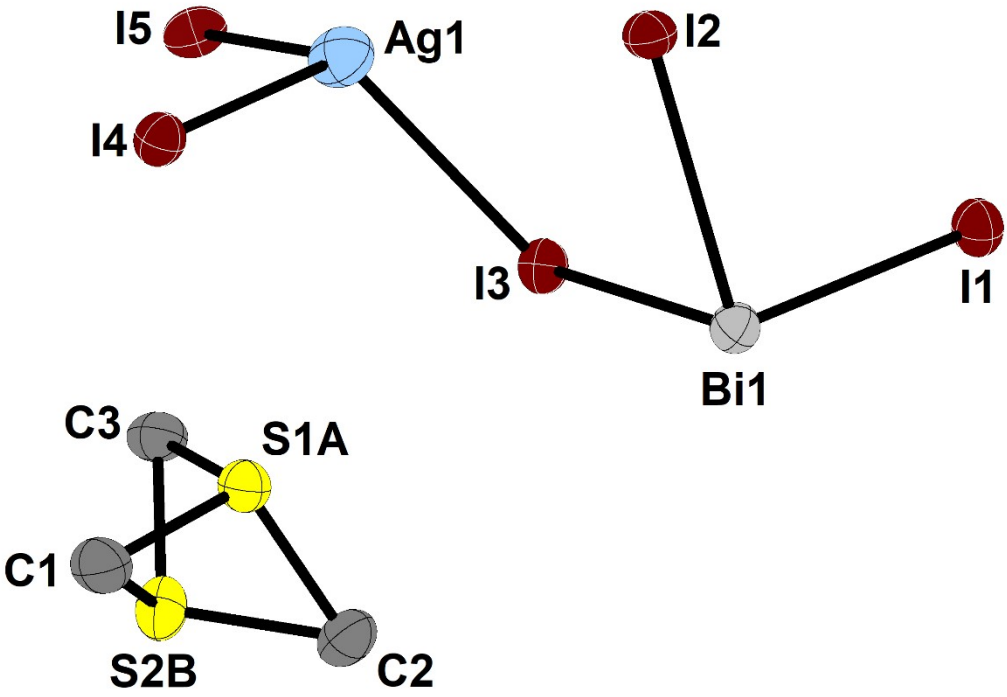

Figure S1: Asymmetric unit of **1**, ellipsoids at 50 % probability. Hydrogen atoms are omitted for clarity.

Table S2: Crystallographic data for **2**, measured on a STOE IPDS2 at 100 K, CCDC 2182490.

	2
Empirical formula	$C_9H_{27}Bi_2I_9S_3$
Formula weight	1791.54
Temperature/K	100
Crystal system	monoclinic
Space group	*C*2/*c*
a/Å	18.9347(13)
b/Å	33.0271(14)
c/Å	22.7116(14)
α/°	90
β/°	91.934(5)
γ/°	90
Volume/Å^3	14194.8(14)
Z	16
ρ_{calc}g/cm^3	3.353
μ/mm^{-1}	17.909
Absorption correction (T_{min}/T_{max})	multi-scan (0.0511/0.1693)
F(000)	12352.0
Crystal size/mm^3	0.0728 × 0.04175 × 0.02221
Radiation	MoK_α (λ = 0.71073)
2Θ range for data collection/°	2.466 to 54.254
Index ranges	-22 ≤ h ≤ 24, -41 ≤ k ≤ 42, -29 ≤ l ≤ 28
Reflections collected	59021
Independent reflections	15293 [R_{int} = 0.1435, R_{sigma} = 0.1738]
Data/restraints/parameters	15293/626/406
Goodness-of-fit on F^2	0.895
Final R indexes [I>=2σ (I)]	R_1 = 0.0626, wR_2 = 0.1272
Final R indexes [all data]	R_1 = 0.1836, wR_2 = 0.1659
Largest diff. peak/hole / e Å^{-3}	1.65/-1.90

Details of crystal structure measurement and refinement: The signal to noise ratio of the dataset is very low, mainly due to small crystal size (see figure S2a/b). Still, there is no doubt about the structural motifs especially when considering that **2** is isostructural to **3** at 293 K.

Of the seven $[SMe_3]^+$-cations in the asymmetric unit two are only occupied with 50 % and three—including one of the only half occupied ones—show a disorder of the sulfur atom over two positions. This disorder in combination with overall quite low reflection intensities made it necessary to refine the carbon positions of residues 1, 2, 4, 6 and 7 as well as S1_7 and S4 isotropically. The positioning of S4 in comparison to the corresponding SMe_3-group (residue 7) as well the size of C2_7 suggests additional disorder in that area. However, this could not be modelled in a better way. With the exception of S4 all carbon-sulfur distances were restraint using SADI commands. Additionally SIMU and

RIGU restraints were used on most of the anisotropically refined carbon and sulfur positions as well as ISOR restraints on C1_5 and C2_5. Initially the SMe_3-groups were modelled using FragmentDB/DSR.[1] Except for the atoms mentioned above all non-hydrogen atoms were refined anisotropically. Hydrogen atoms were assigned to idealized geometric positions and included in structure factors calculations.

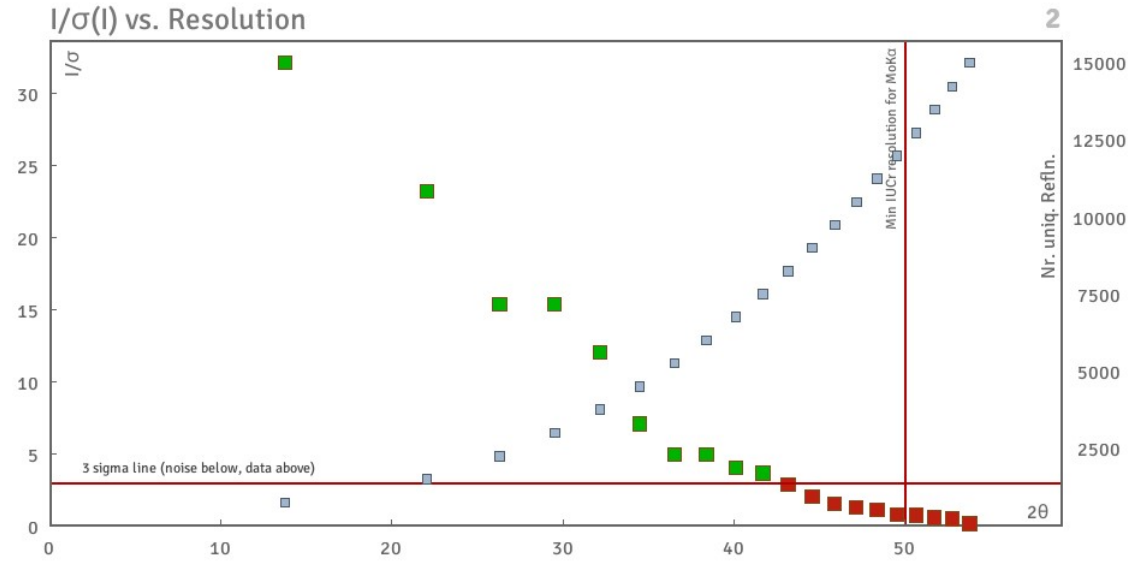

Figure S2a: Plot of the signal to noise ratio against resolution of the x-ray measurement of **2.**

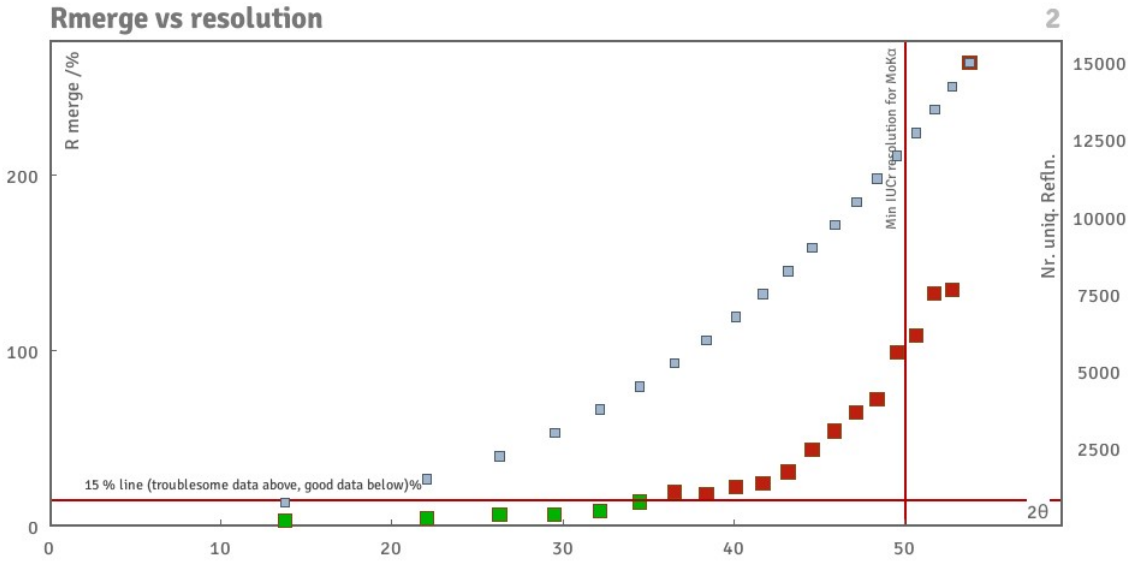

Figure S2b: Plot of the R_{merge} values against of the x-ray measurement of **2.**

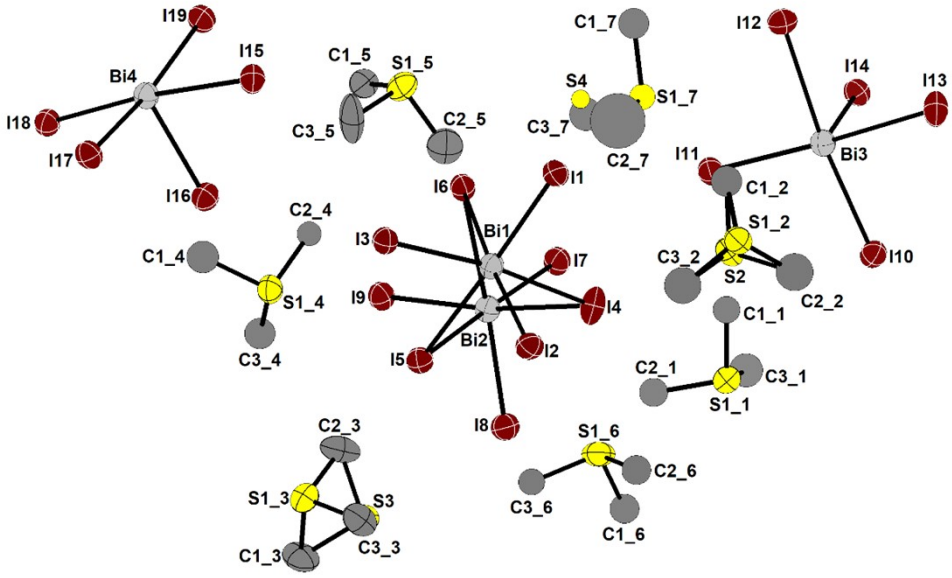

Figure S2c: Asymmetric unit of **2**, ellipsoids at 50 % probability. Hydrogen atoms are omitted for clarity.

Table S3: Crystallographic data for **3**, measured on a STOE IPDS2 at 100 K, CCDC 2182491.

	3
Empirical formula	$C_9H_{27}I_9S_3Sb_2$
Formula weight	1617.08
Temperature/K	100
Crystal system	monoclinic
Space group	*Cc*
a/Å	22.0808(8)
b/Å	9.6940(2)
c/Å	16.2226(6)
α/°	90
β/°	99.086(3)
γ/°	90
Volume/Å^3	3428.90(19)
Z	4
ρ_{calc}g/cm^3	3.132
μ/mm^{-1}	9.860
Absorption correction (T_{min}/T_{max})	numerical (0.1788/0.3134)
F(000)	2832.0
Crystal size/mm^3	0.22929 × 0.15642 × 0.15019
Radiation	MoK_α (λ = 0.71073)
2Θ range for data collection/°	3.736 to 58.574
Index ranges	-30 ≤ h ≤ 30, -13 ≤ k ≤ 13, -18 ≤ l ≤ 22
Reflections collected	29282
Independent reflections	8405 [R_{int} = 0.0557, R_{sigma} = 0.0447]
Data/restraints/parameters	8405/2/217
Goodness-of-fit on F^2	0.945
Final R indexes [I>=2σ (I)]	R_1 = 0.0335, wR_2 = 0.0763
Final R indexes [all data]	R_1 = 0.0442, wR_2 = 0.0795
Largest diff. peak/hole / e Å^{-3}	1.33/-0.83
Flack parameter	0.07(5)

Details of crystal structure measurement and refinement: Initially the SMe_3-groups were modelled using FragmentDB/DSR.[1] All non-hydrogen atoms were refined anisotropically. Hydrogen atoms were assigned to idealized geometric positions and included in structure factors calculations.

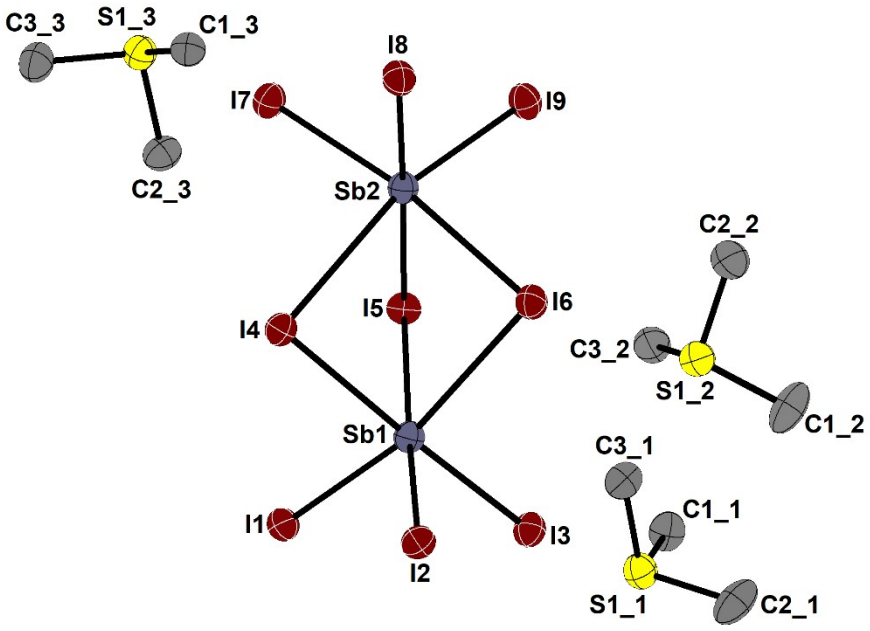

Figure S3: Asymmetric unit of **3** at 100 K, ellipsoids at 50 % probability. Hydrogen atoms are omitted for clarity.

Table S4: Crystallographic data for **3**, measured on a STOE STADIVARI at 293 K, CCDC 2182489.

	3
Empirical formula	$C_9H_{27}I_9S_3Sb_2$
Formula weight	1589.87
Temperature/K	293
Crystal system	monoclinic
Space group	*C*2/*c*
a/Å	19.2137(7)
b/Å	33.5700(18)
c/Å	22.9179(8)
α/°	90
β/°	91.447(3)
γ/°	90
Volume/Å^3	14777.4(11)
Z	16
ρ_{calc}g/cm^3	2.858
μ/mm^{-1}	72.220
Absorption correction (T_{min}/T_{max})	multi-scan (0/0.0025)
F(000)	10896.0
Crystal size/mm^3	0.103 × 0.081 × 0.025
Radiation	CuK_α (λ = 1.54186)
2Θ range for data collection/°	5.266 to 134.998
Index ranges	-22 ≤ h ≤ 15, -40 ≤ k ≤ 39, -27 ≤ l ≤ 27
Reflections collected	55892
Independent reflections	13177 [R_{int} = 0.0699, R_{sigma} = 0.0772]
Data/restraints/parameters	13177/672/482
Goodness-of-fit on F^2	0.882
Final R indexes [I>=2σ (I)]	R_1 = 0.0638, wR_2 = 0.1793
Final R indexes [all data]	R_1 = 0.1430, wR_2 = 0.1954
Largest diff. peak/hole / e Å^{-3}	1.10/-1.01

Details of crystal structure measurement and refinement: Similarly to the isostructural compound **2** all SMe_3-groups show a disorder of the sulfur atom over two positions. The occupancies of the lesser occupied positions vary form 20.7(12) % to 50 %. In the SMe_3-group containing S12, S13, C18, C19 and their symmetry equivalents the group is additionally twisted, leading to overall four carbon positions of 75 % occupancy each. SIMU and RIGU restraints were used on all carbon and sulfur positions as well as ISOR restraints on C3, C7, C10, C11 and C12 to ensure a stable refinement. All atoms were refined anisotropically. Because of the large anisotropic parameters due to the high measurement temperature and the heavy disorder of the SMe_3-groups hydrogen positions could not be refined successfully and therefore were excluded from the final structure.

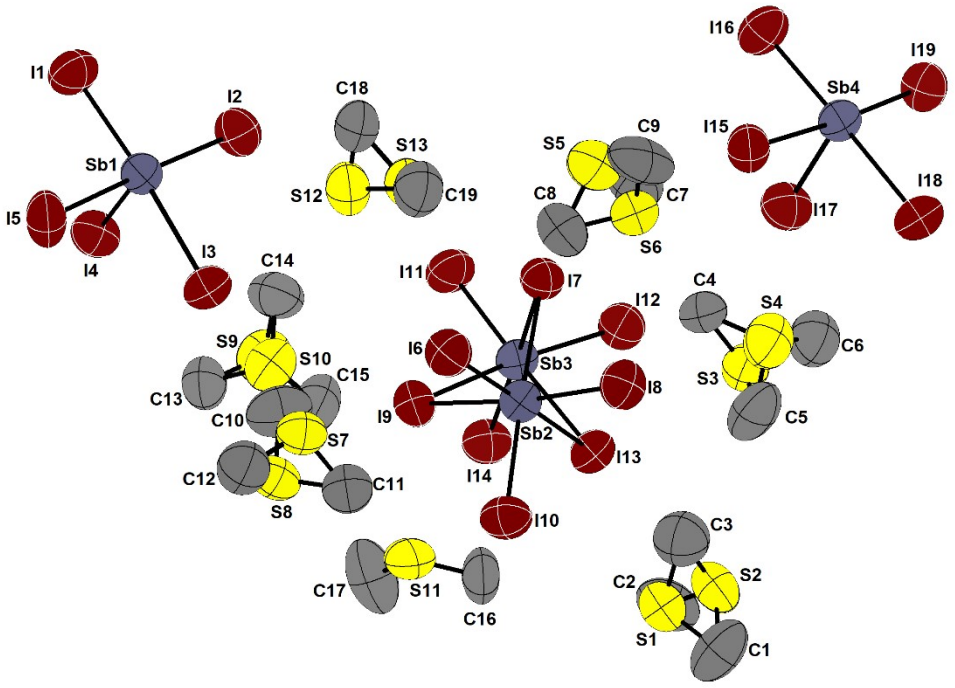

Figure S4: Asymmetric unit of **3** at 293 K, ellipsoids at 50 % probability.

Thermal analysis

The thermal behavior of **1** (2.8 mg), was studied by TGA/DSC on a NETSCH STA 409 C/CD from 20 °C to 1000 °C with a heating rate of 10 °C min^{-1} in a constant flow of 80 ml min^{-1} N_2. Combined TGA/DSC data are shown in figure S5.

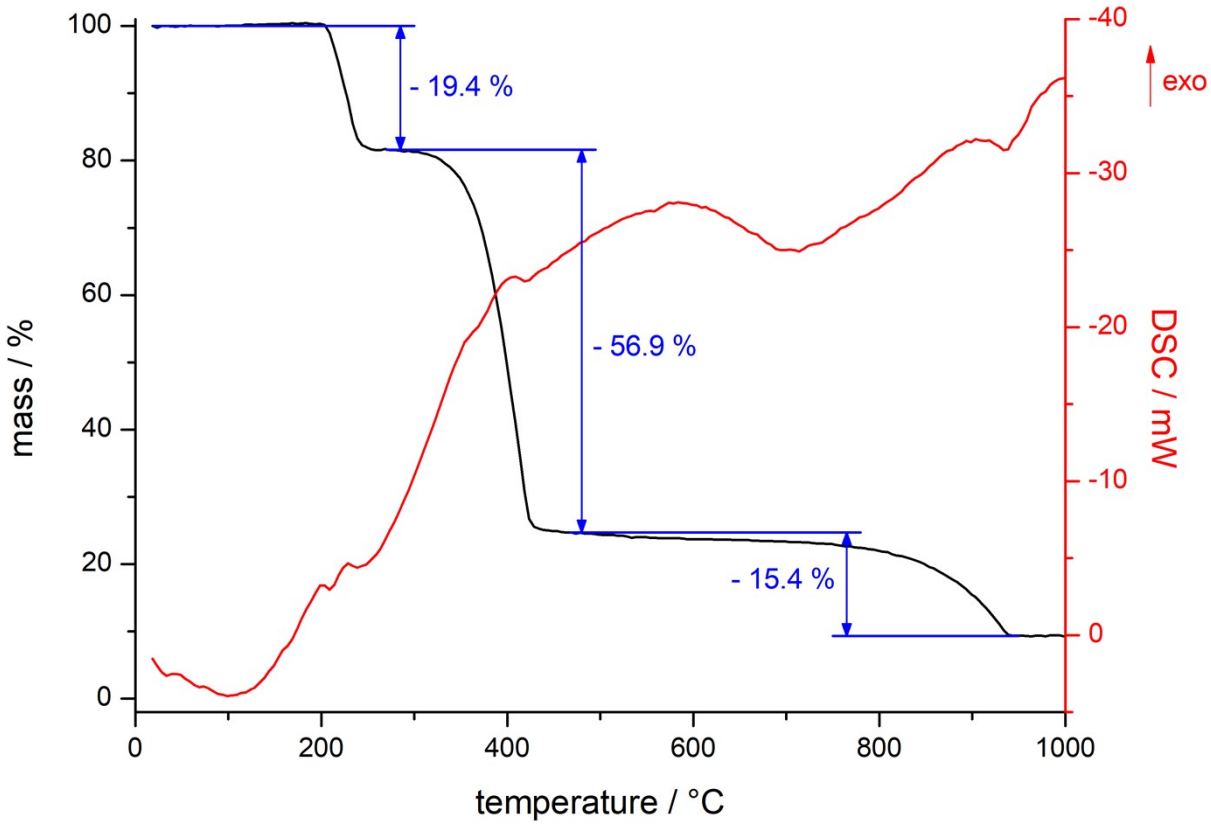

Figure S5: TGA/DSC data for **1.**

The thermal behavior of **2** (14.6 mg), was studied by TGA/DSC on a NETSCH STA 409 C/CD from 20 °C to 1000 °C with a heating rate of 10 °C min^{-1} in a constant flow of 80 ml min^{-1} N_2. Combined TGA/DSC data are shown in figure S6.

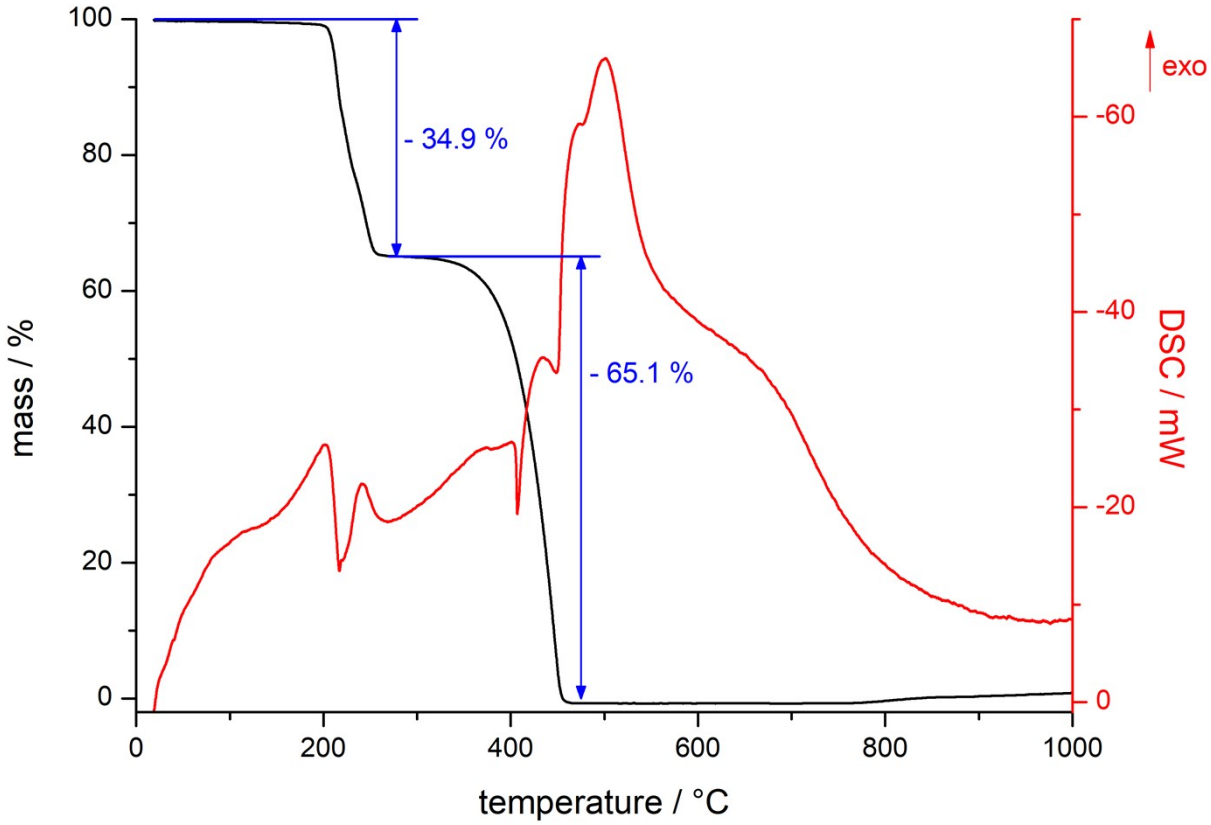

Figure S6: TGA/DSC data for **2.**

The thermal behavior of **3** (19.8 mg), was studied by TGA/DSC on a NETSCH STA 409 C/CD from 20 °C to 1000 °C with a heating rate of 10 °C min^{-1} in a constant flow of 80 ml min^{-1} N_2. Combined TGA/DSC data are shown in figure S7

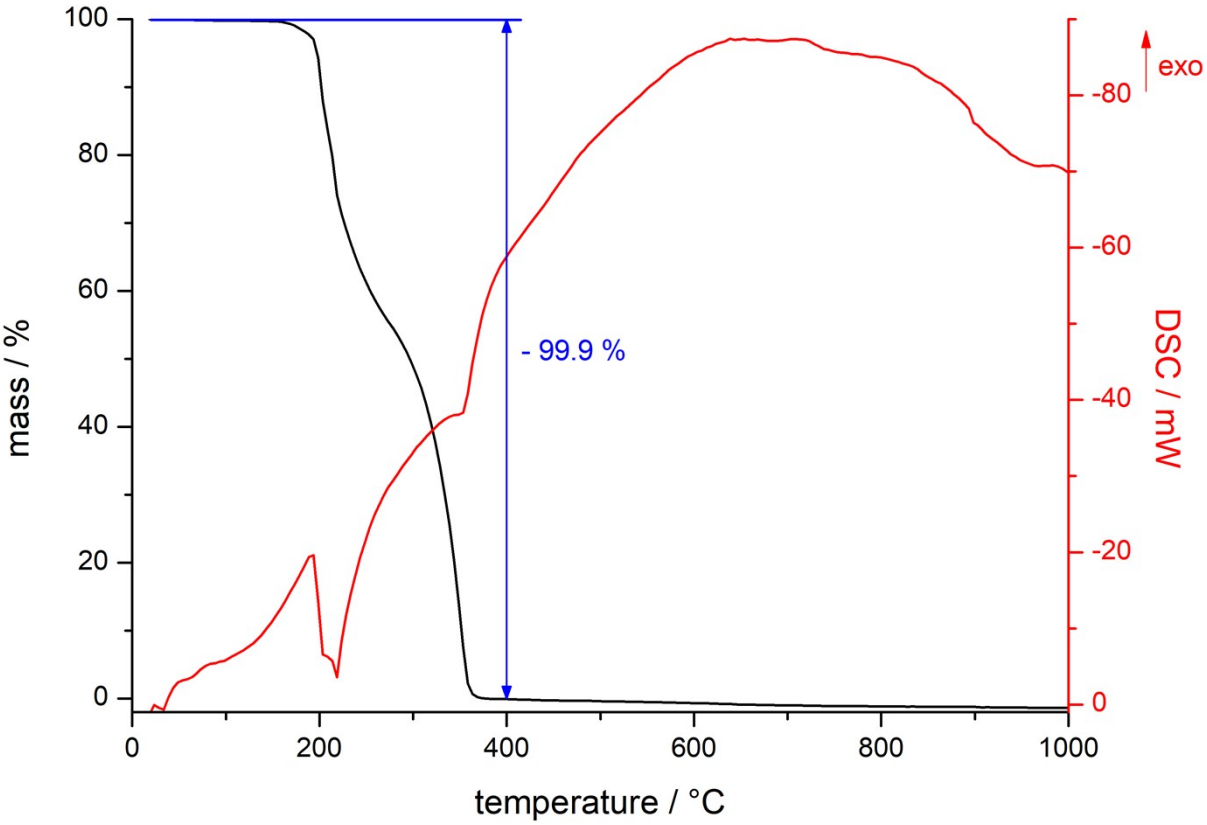

Figure S7: TGA/DSC data for **3.**

Optical properties

Optical absorption spectra were recorded on a *Varian Cary 5000* UV/Vis/NIR spectrometer in the range of 400-800 nm in diffuse reflectance mode employing a Praying Mantis accessory (*Harrick*) with automatic baseline correction.

To determine the optical band gaps the raw data was transformed from reflectance *R* to absorption according to the Kubelka-Munk function

$$F(R) = \frac{(1-R)^2}{2R}$$

and then plotted as a Tauc-plot, where $(F(R) \cdot h\nu)^{1/n}$ is plotted against radiation energy. For a direct band gap n would be $\frac{1}{2}$, for in indirect band bap 2.[2,3] Since the transition in the region of interest was generally far more pronounced when choosing $n = \frac{1}{2}$, we assume that all analysed substances feature an indirect band gap.

The following figures show the reflectance plotted against wavelength as recorded by the spectrometer after baseline correction.

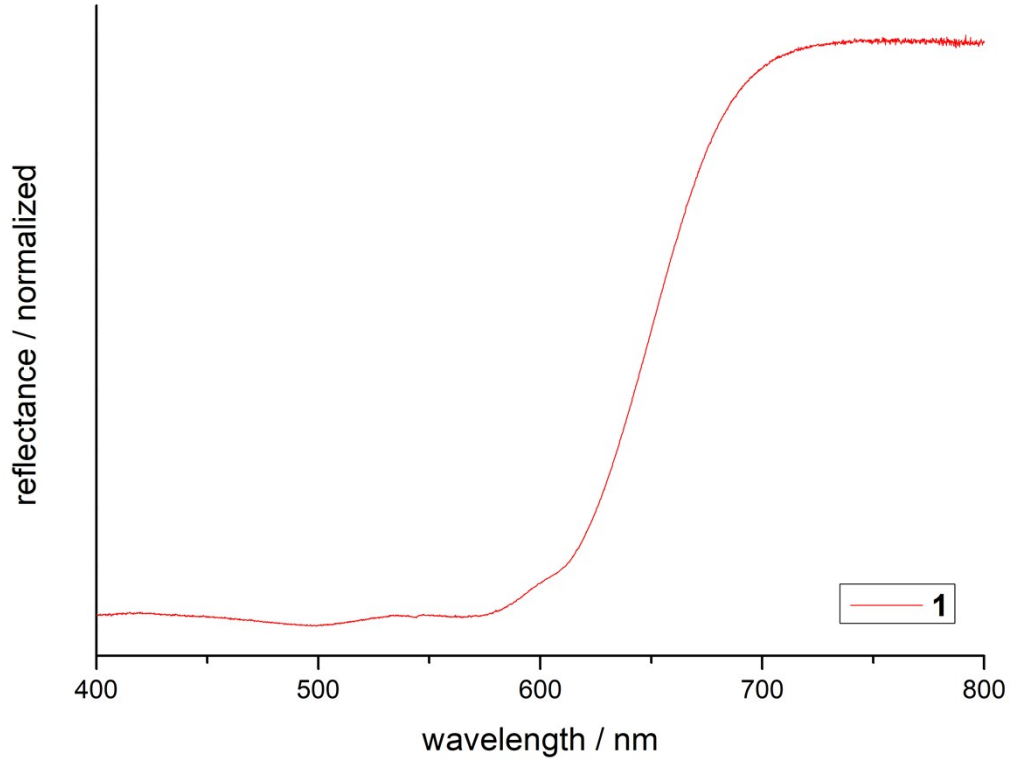

Figure S8. Raw UV-vis data of **1**.

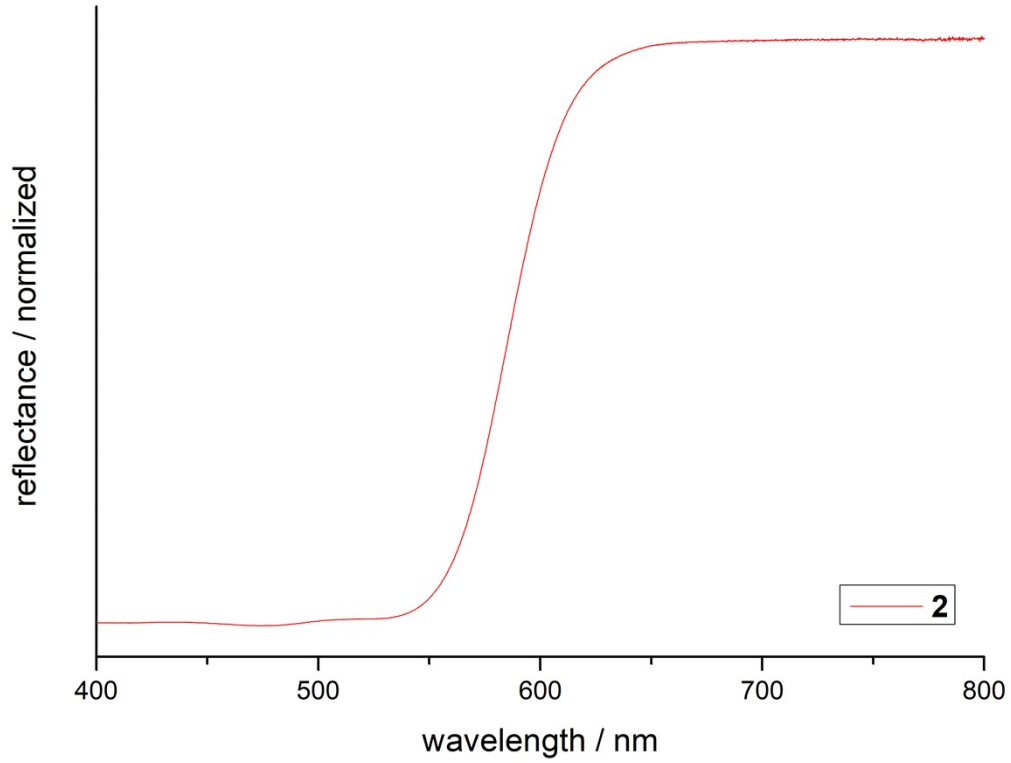

Figure S9: Raw UV-vis data of **2**.

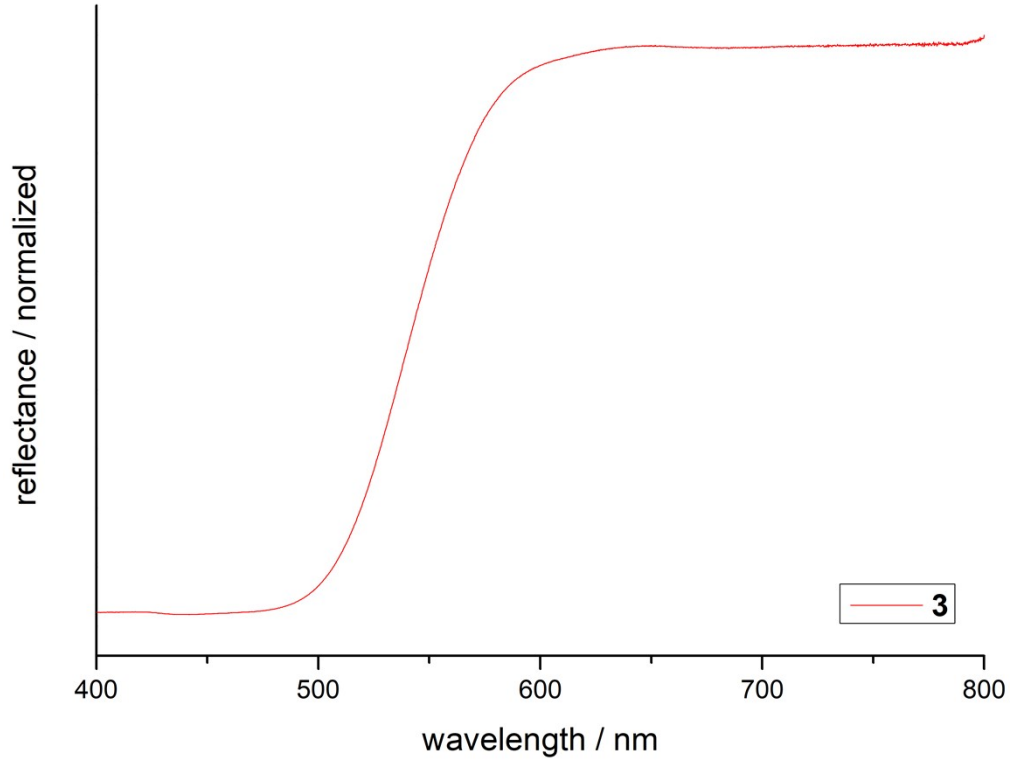

Figure S10: Raw UV-vis data of **3**.

Powder diffraction

Powder patterns were recorded on a *STADI MP* (*STOE* Darmstadt) powder diffractometer with $CuK_{\alpha1}$ radiation with λ = 1.54056 Å at room temperature in transmission mode. The patterns confirm the presence of the respective phase determined by SCXRD measurements and the absence of any major crystalline by-products unless otherwise indicated.

The measured diffractogram of **1** differed significantly from the one initially calculated from SCXRD data showing a preferred orientation. To confirm this and ensure the purity of the crystalline phase a Rietveld refinement was performed using TOPAS-Academic Version 7.[4] Atomic positions of bismuth, silver and iodine atoms were refined freely, a rigid model was used on the disordered SMe_3-group. The preferred orientation was modelled using a spherical harmonics function.

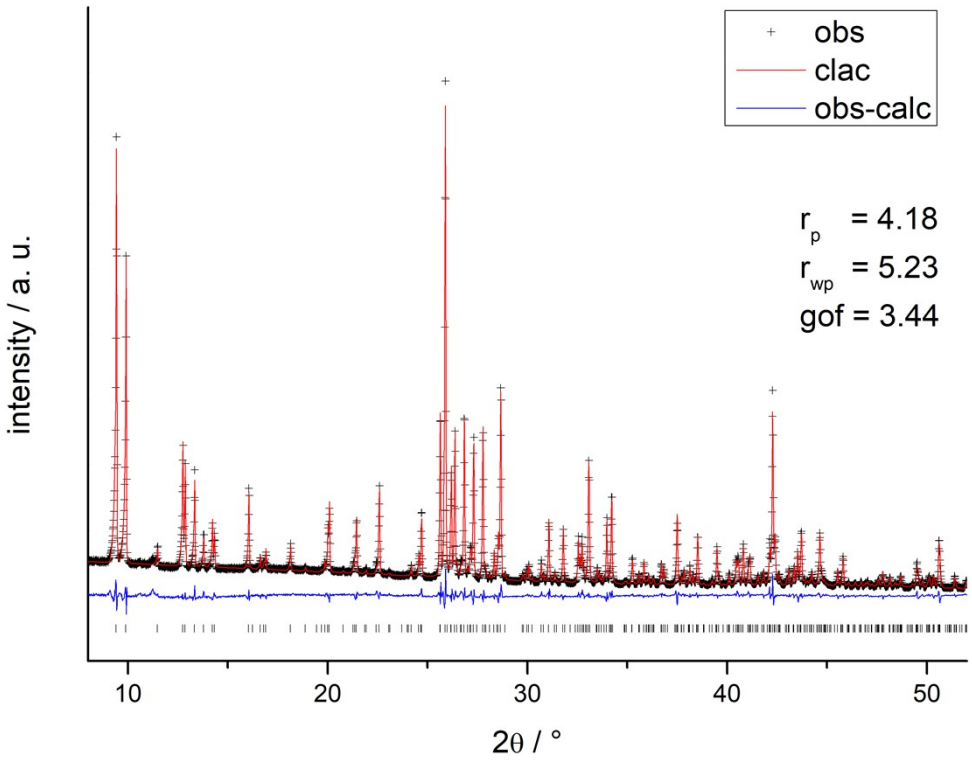

Figure S11: Powder diffraction pattern and results of the Rietveld refinement of **1**.

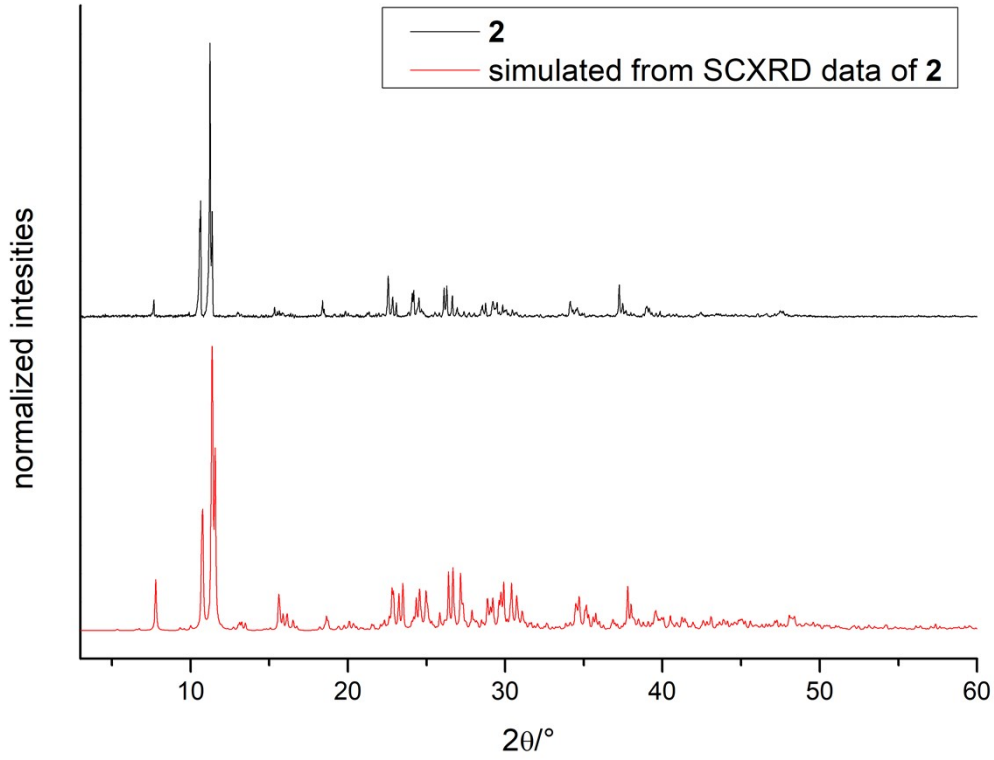

Figure S12: Measured and simulated powder diffraction patterns of **2**.

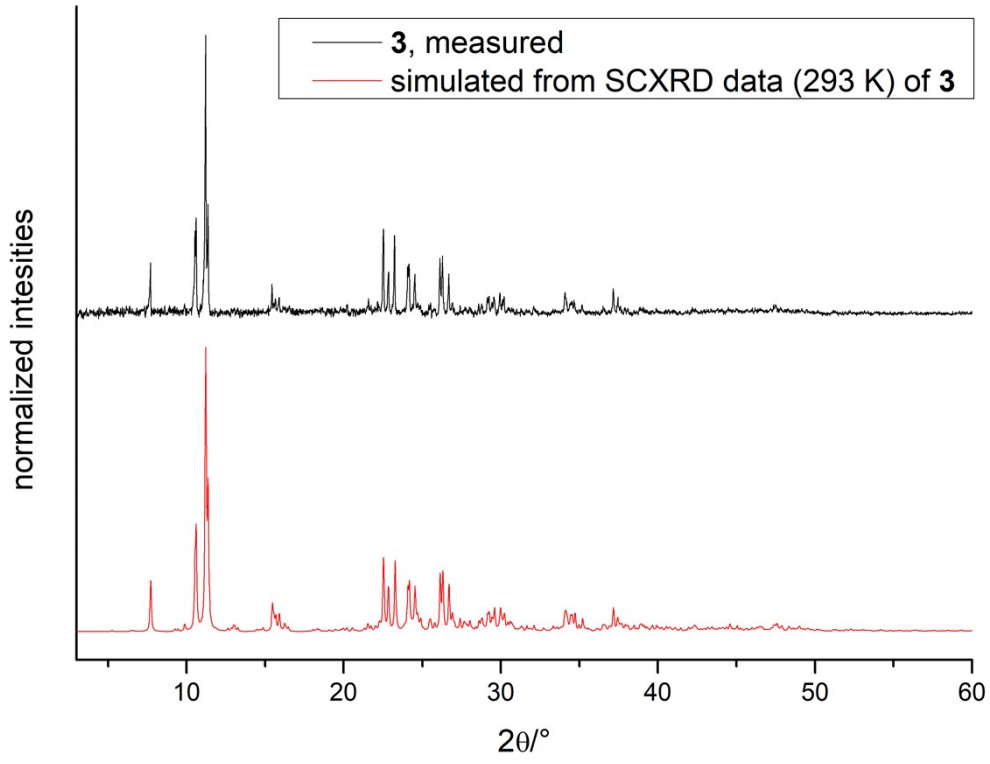

Figure S13: Measured and simulated powder diffraction patterns of **3**.

Computational investigations

Computations were performed using density functional theory (DFT) with periodic boundary conditions using the Vienna Ab initio Simulation Package (VASP 5.4.4).[5-7] The projector-augmented wave (PAW) method was employed in conjunction with the "standard" pseudopotentials for all atoms.[8] Dispersion interactions were included via the DFT-D3 scheme in combination with Becke-Johnson-type damping functions.[9,10] The precision tag was set to "accurate", and a total energy difference of at most 10^{-5} eV was used for SCF convergence. The plane wave energy cut-off was set to 500 eV. For structural optimizations, the generalized gradient approximation (GGA) based exchange-correlation functional proposed by Perdew, Burke, and Ernzerhof (PBE)[11] was used. For band and DOS calculations, spin-orbit coupling (SOC) was also included.[12] For structure optimizations and DOS calculations, a 3x3x3 Monkhorst-Pack k-mesh was used.

All raw data underlying the computations can be found in the free online database NOMAD under DOI: 10.17172/NOMAD/2022.05.23-3

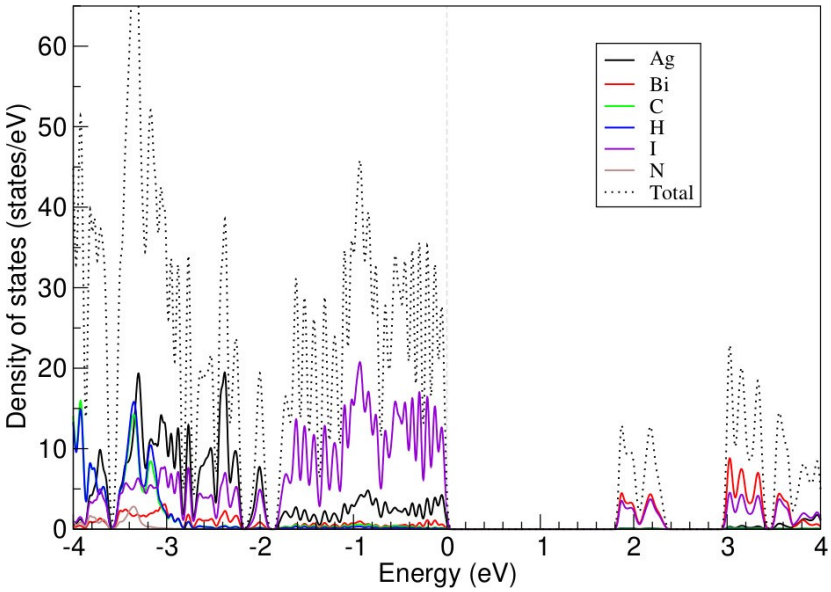

Figure S14. Density of states (DOS) for $[NEt_4]_2[Bi_2Ag_2I_{10}]$ computed at PBE-D3(BJ)/SOC. Shown is the total DOS (dotted line) and the contributions from the elements contained (solid lines). The (indirect) band gap is 1.6 eV.

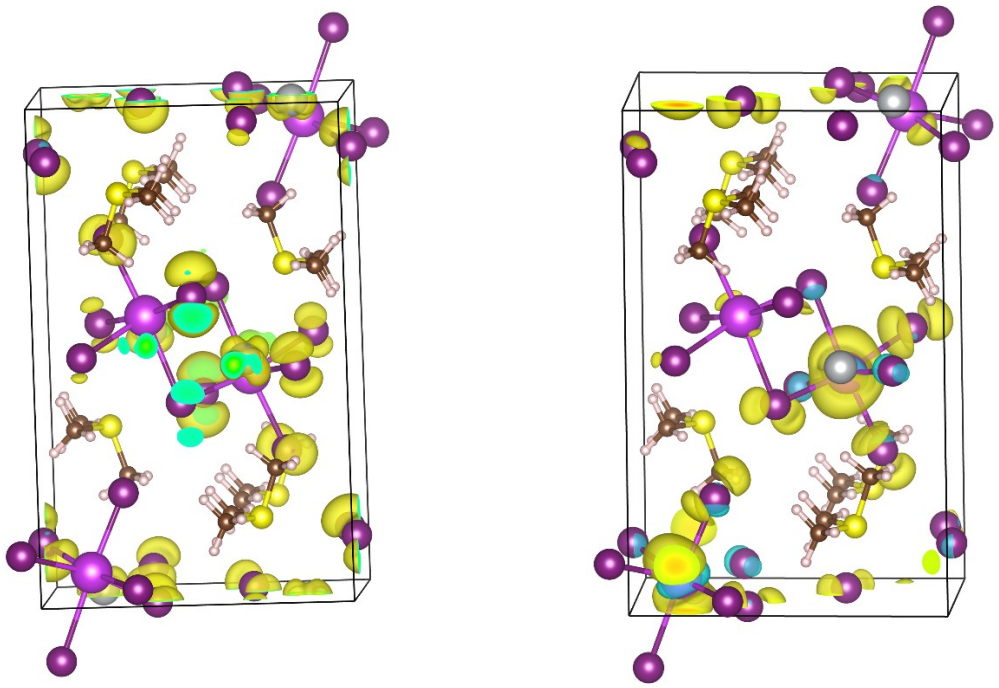

(a) **(b)**

Figure S15. The charge density plot corresponding to (a) valence band and (b) conduction band of complex **1**.

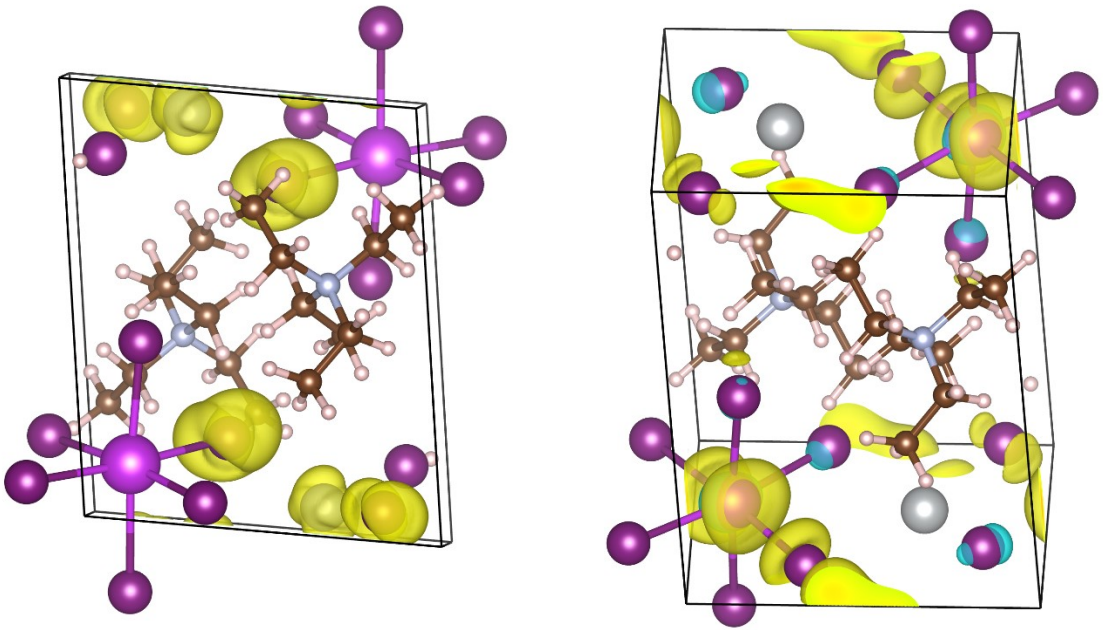

(a) **(b)**

Figure S16. The charge density plot corresponding to (a) valence band and (b) conduction band of $[NEt_4]_2[Bi_2Ag_2I_{10}]$ complex.

Table S5: Crystallographic data for **1** compared to computational results at the PBE-D3(BJ) level.

Lattice parameters	Experimental	Computed	Δ%
a(Å)	8.497	8.528	0.4%
b(Å)	10.930	10.912	-0.2%
c(Å)	17.659	17.394	-1.5%
β(°)	92.05	90.02	-2.2%
Volume (Å^3)	1639.3	1617.7	-1.3%

Table S6: Crystallographic data for $[NEt_4]_2[Bi_2Ag_2I_{10}]$ compared to computational results at the PBE-D3(BJ) level.

Lattice parameters	Experimental	Computed	Δ%
a(Å)	8.822	8.665	-1.8%
b(Å)	10.668	10.509	-1.5%
c(Å)	11.477	11.257	-1.9%
α(°)	92.9	92.2	-0.8%
β(°)	99.7	99.4	-0.3%
γ(°)	97.1	97.9	0.8%
Volume (Å^3)	1053.8	999.8	-5.1%

References

[1] D. Kratzert, J. J. Holstein and I. Krossing, *J. Appl. Crystallogr.*, 2015, **48**, 933.

[2] K. A. Michalow, D. Logvinovich, A. Weidenkaff, M. Amberg, G. Fortunato, A. Heel, T. Graule and M. Rekas, *Catalysis Today*, 2009, **144**, 7.

[3] P. Makuła, M. Pacia and W. Macyk, *J. Phys. Chem. Lett.*, 2018, **9**, 6814.

[4] A. Coelho, *TOPAS-Academic*; Coelho Software, 2020.

[5] G. Kresse and J. Hafner, *Phys. Rev. B*, 1993, **47**, 558–561.

[6] G. Kresse and J. Furthmüller, *Comput. Mater. Sci*., 1996, **6**, 15–50.

[7] G. Kresse and J. Furthmüller, *Phys. Rev. B*, 1996, **54,** 11169–11186.

[8] G. Kresse and D. Joubert, *Phys. Rev. B*, 1999**, 59,** 1758–1775.

[9] S. Grimme, J. Antony, S. Ehrlich and H. Krieg, *J. Chem. Phys.*, 2010, **132**, 154104.

[10] S. Grimme, S. Ehrlich and L. Goerigk, *J. Comput. Chem.*, 2011, **32**, 1456-1465.

[11] J. P. Perdew, K. Burke and M. Ernzerhof, *Phys. Rev. Lett.*, 1996, **77**, 3865–3868.

[12] S. Steiner, S. Khmelevskyi, M. Marsmann and G. Kresse, *Phys. Rev. B*, 2016, **93**, 224425.